A Structural Model for the Kinetic Behavior of Hemoglobin

Keith Moffat, James F. Deatherage, David W. Seybert

Summary. The tertiary structures of all liganded hemoglobins in the R state differ in detail. Steric hindrance arising from nonbonded ligand-globin interactions affects the binding of ligands such as CO and cyanide which preferentially form linear axial complexes to heme; these ligands bind in a strained off-axis configuration. Ligands such as O_2 and NO, which preferentially form bent complexes, encounter less steric hindrance and can bind in their (preferred) unstrained configuration. Linear complexes distort the ligand pockets in the R state (and by inference, in the T state) more than bent complexes. These structural differences between linear and bent complexes are reflected in the kinetic behavior of hemoglobin. Structural interpretation of this kinetic behavior indicates that the relative contributions of nonbonded ligand-globin interactions and nonbonded heme interactions to transition state free energies differ for linear and bent ligands. The relative contributions of these interactions to the free energy of cooperativity may also differ for linear and bent ligands. Thus the detailed molecular mechanism by which the affinity of heme is regulated differs for different ligands.

The details of the molecular pathway by which deoxyHb (*1*) is converted to oxyHb on binding oxygen have proved elusive. Ideally, one would like to identify the molecular processes that control the reactivity of the hemes, both in kinetics and equilibria, and the processes that couple heme ligand binding to the change in quaternary structure. Quantification of these processes in terms of free energy would then provide a structural and thermodynamic basis for ligand binding and cooperativity in hemoglobin. Although the variety and extent of experimental data on hemoglobin exceed that available for any other protein, no such comprehensive molecular mechanism has yet been accepted.

In an attempt to simplify this problem, we have focused on the first set of molecular processes, those that control the reactivity of the hemes within each quaternary structure. This approach originated with Hoard and has been greatly elaborated by Perutz and co-workers. We pose two general questions: What molecular processes control the rates of ligand binding and release, and hence the affinities, of hemoglobin? Can we quantify these processes and provide a structural explanation for their magnitude, for the two quaternary structures, for different ligands, and even for different chains? We consider only briefly the second set of molecular processes which couple ligand binding to quaternary structure; these have been discussed by Baldwin and Chothia (*2*).

Two molecular processes that affect the reactivity of the hemes have been identified: nonbonded heme interactions (*3*, *4*), and nonbonded ligand-globin interactions (*5*). Confusion has resulted concerning the usage of these and the other terms tension at the heme, kinetic cooperativity, stress and strain; we define them explicitly here (*6*). Since the interaction between globin, heme, and ligand is central to these processes, we have undertaken a systematic investigation of the stereochemistry of ligand binding to R-state hemoglobin. We have compared by x-ray difference Fourier techniques the structure of four liganded derivatives of horse Hb–cyanide metHb (*7*), fluoride metHb (*8*), NO Hb (*9*), and azide metHb (*10*) with the structure of the parent compound, acid metHb (*11*), and with the structure of CO Hb (*12*), both determined by Perutz and his colleagues. These six R-state liganded hemoglobins differ in iron spin, ligand bulk, and stereochemistry (Fig. 1). Here we present a comparison of their structures, and emphasize the small but significant differences in tertiary structure between them (*13*). This difference Fourier approach is more sensitive to small structural changes (*14*) than the necessarily indirect superposition of the deoxyHb, acid metHb, and CO Hb dimers presented by Baldwin and Chothia (*2*). We can readily detect structural changes in the globin and the heme that exceed 0.2 Å and 0.1 Å, respectively: their corresponding figures are ~ 0.6 Å and ~ 0.35 Å [table 1 in (*2*)]. Baldwin and Clothia concentrate on the larger tertiary structural changes that accompany change in ligation and the R-T quaternary structural transition; we identify the smaller but related changes that accompany alteration in the ligand without change in quaternary structure. The two sets of results are therefore complementary.

From these and other crystallographic results, we propose a model to account for *kinetic* differences between ligands in structural terms. This is a novel approach, since previous studies (*5*, *15*) have been largely focused on *equilibrium* properties. It is also hazardous, since kinetic rate constants ultimately depend on the difference in free energy between stable, crystallographically observable structures such as deoxyHb or CO Hb, and transient, unobservable structures of the transition states for the reaction. We are encouraged to take this approach because a dissection of ligand equilibrium constants into association and dissociation rate constants emphasizes the different contribution of steric and electronic factors to each, and because a particularly striking correlation between the stereochemistry of the heme-ligand complexes and the kinetic properties of the association reactions emerges, which is both chemically and structurally plausible.

Comparison of the Crystal Structures of Liganded Horse Hemoglobins

Each of the structures of NO Hb, cyanide metHb, azide metHb, fluoride metHb, and CO Hb has been compared individually with the structure of acid metHb (*7–10*, *12*). With the sole exception of fluoride metHb (which we do not consider further), these differ both in the stereochemistry of the heme and in

Dr. Moffat is an associate professor and Drs. Deatherage and Seybert were graduate students, in the Section of Biochemistry, Molecular and Cell Biology, Cornell University, Ithaca, New York 14853. Dr. Deatherage's present address is MRC Laboratory of Molecular Biology, Hills Road, Cambridge, England; Dr. Seybert's present address is Department of Chemistry, Duquesne University, Pittsburgh, Pennsylvania 15219.

0036-8075/79/1130-1035$02.00/0

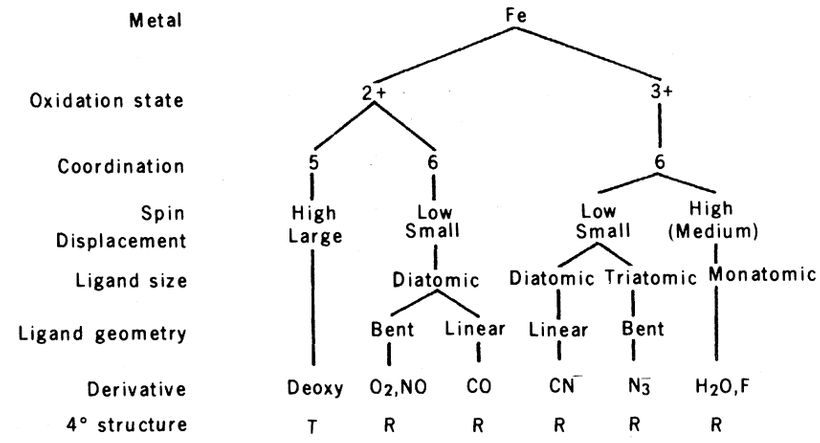

Fig. 1. Classification of liganded hemoglobin derivatives. Displacement refers to the distance of the iron from the mean porphyrin plane. The structures of these derivatives (with the exception of oxyHb, which is not known) are presented in (*7–12, 22*).

the tertiary structure of the globin from acid metHb.

Comparisons between these structures show that they differ significantly one from another. That is, all liganded hemoglobins so far examined differ in tertiary structure; they cannot be assumed to be structurally equivalent. As an example, difference electron density sections through the β hemes of NO Hb, cyanide metHb, and azide metHb are shown in Fig. 2, a to c. These differ one from another; however, the α and β hemes for the same ligand are more similar [compare Fig. 2a with figure 6 in (*9*) and Fig. 2c with figure 5 in (*10*)].

These differences in heme stereochemistry are coupled to differences in tertiary structure of the globin in the ligand and heme pockets, and in the $\alpha 1\beta 2$ interface. Some of the more striking differences, summarized in Table 1, have been described (*7–10, 12, 16*). Studies in solution by such techniques as nuclear magnetic resonance and infrared and Raman spectroscopy have also shown that there are tertiary structural differences between liganded hemoglobins and between the α and β chains for the same ligand (*17*). Quantification in structural terms of these spectroscopic differences has generally not been possible, although it can now be aided by the determination of the related crystal structures. We focus on the two components of these tertiary structural differences most directly related to kinetic behavior: the stereochemistry of ligand binding, and the conformation of the heme and ligand pocket.

Stereochemistry of Ligand Binding

From studies of heme structure, a general principle has emerged which is relevant to the structure of liganded hemoglobins. We adopt the convention of Enemark and Feltham (*18*), and denote a given porphyrin metal (M)—diatomic ligand (XY) system by $[MXY]^n$, where n is the sum of the number of d electrons on the metal together with only those electrons on the XY ligand which occupy the π^* or σ^* levels. For example, we have $[Fe(II)CO]^6$, $[Fe(III)CN^-]^6$, $[Mn(II)NO]^6$, $[Fe(II)NO]^7$, $[Fe(II)O_2]^8$, and $[Co(II)O_2]^9$. Crystallographic studies of such externally unconstrained metalloporphyrins have shown (*19*) that for $n = 6$, a linear end-on structure for the metal-ligand complex is preferred, in which the diatomic ligand lies along the heme axis (the normal to the mean porphyrin plane passing through the metal); as n increases through 7, 8, and 9, a progressively more bent end-on structure is preferred. Thus for $[Fe(II)CO]^6$, the M-X-Y bond angle (denoted θ in Table 2) is 180°; for $[Mn(II)NO]^6$, it is 176°; for $[Fe(II)NO]^7$, it is 142°; and for $[Fe(II)O_2]^8$, it is 129° (*19*). The theoretical basis for this progressive change in stereochemistry is reasonably well understood (*20*). We may therefore anticipate that the corresponding ligands in hemoglobin and other heme proteins would adopt a similar structure, provided that they were externally unconstrained.

To examine this point, we obtained the conformation of the ligands by model building into derivative electron density maps of NO Hb, cyanide metHb, and azide metHb (Table 2). Despite the quantitative limitations of this approach (*9*), the crucial qualitative result is clear: the ligand stereochemistry in both NO Hb and azide metHb [where a bent end-on structure is also predicted (*19*)] is consistent with that found in externally unconstrained metalloporphyrins; for cyanide metHb and CO Hb, it is not consistent. In all four derivatives, the ligand density corresponding to the second ligand atom is significantly displaced off the heme axis and lies roughly over pyrrole II, with the orientation angle ϕ around 200° (Fig. 2 and Table 2). A similar off-axis distortion of the "linear" cyanide or CO ligands has been observed in the other heme proteins—myoglobin, erythrocruorin, and lamprey hemoglobin (*21*). With the exception of cyanide metHb (*7*), these results were uniformly interpreted in terms of bent cyanide or CO ligand, although we have suggested that a reinterpretation in terms of a basically linear but distorted ligand is to be preferred [see figure 6e of (*7*)] in that theoretical studies (*20*) suggest that it is energetically expensive to bend the linear ligands but relatively inexpensive to distort the porphyrin normal to its mean plane (*19*).

The reason for this distortion of the linear ligands is clear. Table 2 also lists the nonbonded interaction distances between ligand atoms and surrounding globin residues in the heme pocket, with the refined coordinates of acid metHb. Were cyanide and CO to be linear and lying along the heme axis, they would make

Table 1. Main tertiary structural differences between the liganded hemoglobins and metHb in the R state. The plus sign indicates the change described is observed; the minus sign indicates the change opposite to that described is observed; 0 indicates no change is observed; parentheses indicate uncertain.

Structural feature	Cyanide metHb		CO Hb		NO Hb		Azide metHb	
	α	β	α	β	α	β	α	β
Distorted ligand	+++	+++	+++	+++	0	0	0	0
Distal histidine shift away from ligand	++	++	+++	+++	++	+++	+	++
Ligand pocket expansion; E and B helices away from heme	++	+++	(0)	+	0	+	−	+
Iron motion to distal	+	0	+	++	++	++	0	0
Porphyrin motion to distal	(+)	0	+	+	++	++	0	0
Heme tilt	++	+++	++	++	0	+	0	0
F helix shift toward heme	+	++	0	++	0	+	+	+
Tyrosine HC2 expelled from pocket	0	+	0	+++	0	−	0	+
Valine FG5 shift toward $\alpha 1\beta 2$	+	+	0	0	0	−	0	0

unacceptably short contacts with certain globin residues, in particular with histidine (His) E7 and valine (Val) E11 these short contacts may be relieved by distorting the ligand, the heme, and the heme pocket (*7, 12*). No such short contacts are made by the bent ligands NO and azide, and little or no distortion is necessary [although His E7 is displaced in all derivatives (Table 2)]. These short contacts are particularly acute in the β chains, where the ligand pocket of acid metHb is appreciably smaller than in the α chains (*11*). This effect is even further accentuated in the deoxyHb T structure, where the ligand binding site is almost completely occluded in the β chain by the side chain of Val E11 (*22*).

Conformation of the Heme and the Ligand Pocket

The conformation of the heme and the ligand pocket differs in all the liganded derivatives (Fig. 2 and Table 1). Again on the basis of the structures of the corresponding free hemes (*19*), some differences in heme conformation were anticipated since cyanide, azide, NO, and CO all form low-spin complexes with iron; but water, the ligand in acid metHb, forms a largely high-spin complex with iron, with only a small amount of low-spin component in equilibrium with it (Fig. 1). In model five-coordinate high-spin ferric (and ferrous) complexes, the iron lies out of the plane of the pyrrole nitrogens, by up to 0.5 Å; in low-spin complexes, the iron lies in or very near the plane of the pyrrole nitrogens. Relative motion of the iron and the pyr-

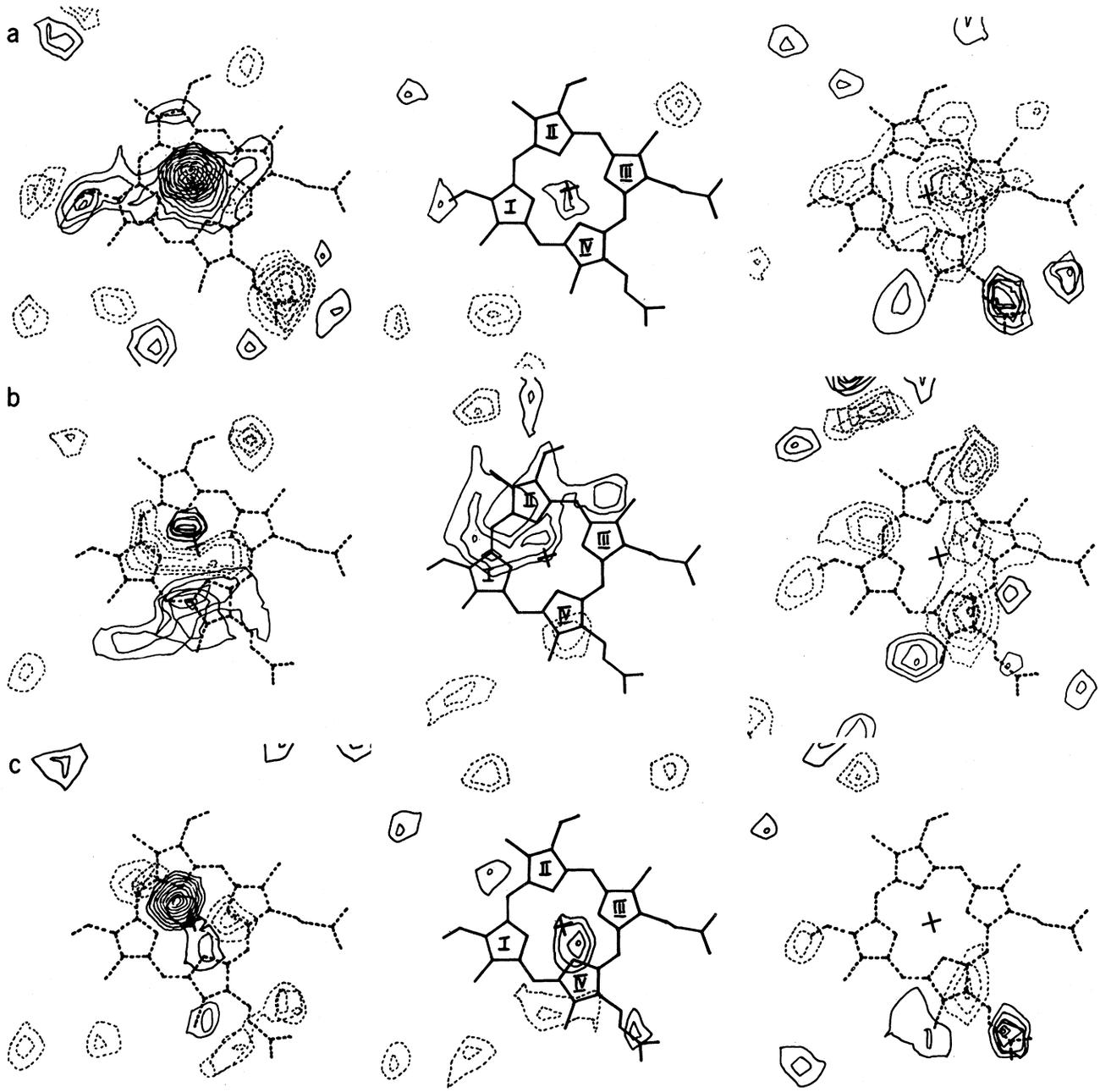

Fig. 2. Sections through the difference electron density maps parallel to the β hemes. Positive contours, solid; negative contours, dashed; contour interval 0.02 electron/Å^3. The zero and the first positive and negative contours have been omitted. The projection of the heme is shown in outline, with the pyrrole numbering. (Left) Sections 1 Å and 2 Å distal to the heme; (center) section in the plane of the heme; (right) sections 1 Å and 2 Å proximal to the heme. (a) NO Hb–metHb; (b) cyanide metHb–metHb; (c) azide metHb–metHb. The differences in tertiary structure in the globins may be noted by comparing figures 1 to 5 in (*7*), figures 1 to 4 in (*8*), figures 1 to 4 in (*9*), and figures 1 to 4 in (*10*).

role nitrogens was therefore anticipated when we compared the low-spin derivatives with acid metHb. We were therefore surprised to find that, with the possible exception of the NO (and CO) derivatives in the β chain, no difference electron density unambiguously attributable to motion of the iron could be detected (Table 1); even with NO and CO derivatives, the motion is unexpectedly small, about 0.1 Å. Motion of the pyrrole nitrogens occurred in some derivatives (Table 1) (*16*); but no uniform trend was observed. Similar results have been obtained on other heme proteins (*21*). These findings have been clarified by the recent determination of the structure of the first six-coordinate high-spin ferric porphyrins (*23*) which showed that, contrary to prior expectations, the iron was exactly centered in the plane of the pyrrole nitrogens. The larger high-spin iron was accommodated by radial expansion of the porphyrin core, enlarging the central hole.

Detailed examination of the heme conformation in heme proteins is hindered by the limited resolution of the x-ray data. Also, crystallographic refinement of the hemes in acid metHb, deoxyHb, deoxyMb, and acid metMb (*11, 22, 24*) did not distinguish between planar and domed hemes, and therefore they were assumed to be planar. However, ruffled geometries in which the methene carbons lie alternately proximal and distal to the mean porphyrin plane were not considered (*25*), although this form of strain is frequently found in hemes (*19*).

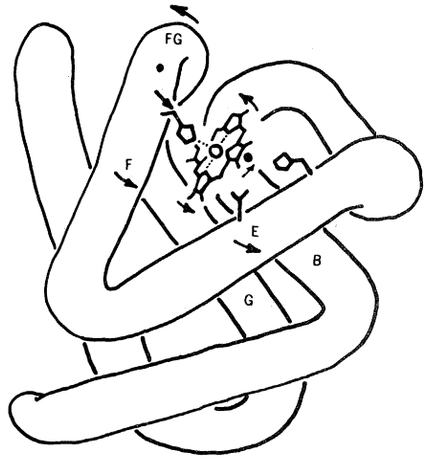

Fig. 3. The tertiary structure change on ligand binding in the R state, illustrated by an isolated β chain. This change is seen most clearly in the cyanide metHb difference Fourier, but traces of it are seen in the other derivatives.

Should ruffling be detected by further crystallographic refinement, revision of the heme coordinates will be required. In any case, our results show that the hemes do not have an unstrained axially symmetric conformation in at least some liganded hemoglobin derivatives, and that there is no direct correlation between heme strain and spin state. We conclude that heme stereochemistry is significantly influenced not merely by the properties of the iron, but also by constraints imposed by the protein.

Conversely, the conformation of the globin is influenced by the heme-ligand conformation either directly through nonbonded ligand-globin interactions, or indirectly through heme-globin interactions which depend on the tilt and location of the heme. Although the details of these interactions are complex (*16*), the tertiary structural changes important for our subsequent discussion may be briefly summarized (Table 1). On ligand binding to R-state hemoglobin (or substitution of bulkier ligands for the water ligand in acid metHb), the most prominent effects are expansion of the ligand pocket (movement of the distal histidine and E helix away from the heme in response to a change in the ligand bulk), movement of the F helix (toward the heme in response to change in iron-nitrogen bond lengths) and tilting of the heme (*26*). Closely related tertiary structural changes occur on ligand binding to deoxyHb constrained in the T state (*27*). These tertiary structural changes which occur within the R and T quaternary structures without change in quaternary structure appear to be qualitatively similar to, but smaller in magnitude than, those tertiary structural changes which accompany the R-T change in quaternary structure (*2*).

In R-state hemoglobin, both ligand pocket expansion and heme tilt are largest for the linear cyanide ligand, and smaller or absent for the bent NO and azide ligands; they are also somewhat larger in the β chain than in the α chain, again consistent with the smaller size of the ligand pocket in the β chain than in the α chain of acid metHb (*11*). In view of the numerous close contacts between the heme and the globin, it is not surprising that heme tilt is closely coupled to motion of the globin. Indeed, the magnitude and extent of the overall change in tertiary structure, shown schematically for cyanide metHb in Fig. 3, is roughly correlated with the magnitude of the heme tilt, being larger in cyanide metHb than in NO Hb or azide metHb. Movement of the pyrrole IV edge of the heme is linked to E and F helix movement, and movement of the pyrrole II edge of the heme is linked to movement of the F helix and FG corner. Movement of the inner heme edge is linked to movement of G and H helix side chains lining the heme pocket. Lesser structural effects are movement of the D and B helices (in response to movement of the E helix), pivoting of the G helix (in response to movement of the B helix, the inner heme edge, and the FG corner), and shifts of the H helix (in response to movement of the F and G helices and perhaps the heme). These heme-linked changes in tertiary structure extend to the $\alpha 1\beta 2$ interface. Reversal of these changes on release of

Table 2. Approximate ligand stereochemistry in hemoglobin. The approximate ligand conformations were deduced by fitting to derivative electron density maps (*9*). L_1 and L_2 denote the first and second ligand atoms; θ denotes the angle Fe-L_1-L_2; ϕ denotes the angle between the line Fe-N of pyrrole IV and the projection of the line L_1L_2 on the porphyrin plane. The distances Fe-L_1 and L_1-L_2 were fixed at the values in appropriate model compounds (*19*), and the porphyrin and globin coordinates were fixed at those of metHb (*11*); θ and ϕ were then varied. The estimated error in θ and ϕ is $\pm$ 10°, and in the contact distances is $\pm$ 0.2 Å. These errors are in large part due to motion of the porphyrin and globin in the derivatives (Table 1) and to uncertainties in the true heme coordinates (*25*). The short contact distances to His E7 are relieved by its motion away from the ligand (Table 1). The data for an inclined model for CO, and a prediction for bent O_2, are taken from (*12*).

Ligand	Fe-L_1 (Å)	L_1-L_2 (Å)	θ (deg)	ϕ (deg)	Distance (Å) from L_2 to:	
					N_ϵ His E7	$C_{\gamma 2}$ of Val E11
α chain						
Cyanide	1.84	1.14	160	205	2.5	3.6
CO	1.84	1.14	(140)	166	(3.5)	(4.0)
NO	1.74	1.12	145	205	2.9	3.7
O_2	1.75	1.24	136	170	3.1	3.7
Azide	1.93	1.35	125	195	3.3	4.1
β chain						
Cyanide	1.84	1.14	150	200	2.9	3.2
CO	1.84	1.14	(140)	226	(2.9)	(3.9)
NO	1.74	1.12	145	195	2.7	3.4
O_2	1.75	1.24	136	190	2.9	3.4
Azide	1.93	1.35	125	200	3.4	3.5

ligand from R-state hemoglobin ultimately leads to the change in quaternary structure to the T state (*2, 16*).

Three key points from these results will be used in our kinetic model: the geometry of externally unconstrained heme-ligand complexes $[MXY]^n$ depends on the value of n, and may be distinguished as either linear or bent; in heme proteins, linear heme-ligand complexes are considerably distorted from their preferred unconstrained geometry, but bent complexes are not; and the ligand pockets are also distorted in linear complexes, but only to a much lesser extent in bent complexes.

Structural Model for Hemoglobin Kinetic Behavior

A detailed molecular mechanism of action for hemoglobin has been based on the extensive structural and equilibrium data available (*5, 15*). Two molecular processes were proposed to account for the lowered ligand affinity of deoxyHb: the change in heme stereochemistry which accompanies the transition of the iron from five-coordinate high spin (as in deoxyHb) to six-coordinate low spin (as in oxyHb), and a change in the conformation of the heme pocket that increases distal steric hindrance to ligand binding.

The first process was proposed to lower the affinity through "tension at the heme" (*5, 6*) in the T quaternary structure, where the globin exerts stress along the line of the proximal histidine-to-iron bond, moves the iron further out of the plane of the pyrrole nitrogens, and strains the heme. This stress opposes motion of the iron into the mean plane of the pyrrole nitrogens and its combination with ligands. The additional iron displacement normal to the mean plane of the porphyrin on which this process was based (*5*) has not been substantiated by crystallographic refinement (*2, 22*) or by other measurements (*4, 28*). However, dramatic evidence for *some* stress in the T state on the liganded heme was provided by the demonstration that inositol hexaphosphate binding to NO Hb not merely switched its quaternary structure from R to T, but also ruptured (or at least greatly stretched) the iron to proximal histidine bond of the α heme, but not the β heme (*29*). Related evidence for stress on the α heme, greater than that on the β heme, was obtained by Sugita (*30*) from studies of hybrid hemoglobins in which the α and β chains contained spectrally distinct hemes, proto- and mesoheme. It has been shown that the proximal histidine in deoxyHb is asymmetrically located with respect to the pyrrole nitrogens, but this asymmetry is absent in liganded hemoglobins (*2, 4*). This novel form of heme strain does not reflect much stress in the unliganded T state; rather, it contributes to lowered ligand affinity through repulsive nonbonded heme interactions in the liganded T state (*2, 4*).

The view which emerges from these studies is that tension at the heme as originally defined (*5*) does not contribute to lowered ligand affinity; stress on the heme through nonbonded heme interactions is most pronounced in the α chain in the T quaternary structure; and its effects on ligand affinity arise from destabilization of the liganded T state.

The possible influence of tension at the heme on ligand affinity has been closely examined; but the second process noted by Perutz (*5*), distal steric hindrance to ligand binding, has received less attention. On the basis of our structural results and the kinetic data presented below, we propose (*16, 31*) the following.

1) Steric hindrance to ligand binding through nonbonded ligand-globin interactions is an additional and significant source of the lowered ligand affinity of deoxyHb in the T quaternary structure.

2) Steric hindrance is present to a lesser extent in the R quaternary structure and single-chain heme proteins.

3) The extent of steric hindrance differs between linear (as in CO) and bent (as in NO and O_2) ligands, and is consid-

Table 3. Kinetics of ligand binding by monomeric heme proteins and free hemes. The variables x' and x denote association and dissociation rate constants in units of liters per micromole per second and per second, respectively. Most data for heme proteins were obtained in 0.1 *M* phosphate, *p*H 7, at 20°C; those for free hemes in 2 percent cetyltrimethylammonium bromide suspension were obtained in 0.15*M* phosphate, *p*H 7.3, at 20°C. Data for $[Fe(II)O_2]^8$ and $[Fe(II)CO]^6$ are taken from (*45*); for $[Fe(II)NO]^7$ from (*46*); for $[Co(II)O_2]^9$ from (*47*); and for free hemes, from (*33, 34, 48*). The free hemes selected are all those with imidazole or l-methylimidazole bases, without strain, and for which both CO and O_2 kinetic data exist.

Protein or heme	Constant	Linear ligand complex	Bent ligand complexes			Ratio x'_{bent}/x'_{linear}
		$[Fe(II)CO]^6$	$[Fe(II)NO]^7$	$[Fe(II)O_2]^8$	$[Co(II)O_2]^9$	
Mb (sperm whale)	x'	0.5	17	19	40	34 to 80
	x	1.7×10^{-2}	1.2×10^{-4}	10	2.8×10^{3}	
Mb (*Aplysia*)	x'	0.5		15		30
	x	2.0×10^{-2}		70		
α^{SH}	x'	4.0	24	50		6 to 12
	x	1.3×10^{-2}	4.6×10^{-5}	28		
β^{SH}	x'	4.5	24	60		5 to 13
	x	8.0×10^{-3}	2.2×10^{-5}	16		
α^{PMB}	x'	3.9		55		14
	x	1.6×10^{-2}		31		
β^{PMB}	x'	2.4		80		33
	x	2.7×10^{-2}		156		
Free hemes	x'	3.5 to 30	80	22 to 60		1.5 to 8
	x	6.5×10^{-3} to 1.9×10^{-2}		23 to 44		

Table 4. Kinetics of ligand binding by the T (deoxy) and R (liganded) states of human hemoglobin. Association and dissociation rate constants x' and x are expressed in units of liters per micromole per second and per second, respectively. Most data were obtained in 0.05*M* phosphate, *p*H 7, 20°C. Data for $[Fe(II)O_2]^8$ are taken from (*36*); those for $[Fe(II)NO]^7$ are from (*46*); those for $[Fe(II)CO]^6$ are from (*49*); and those for $[Mn(II)NO]^6$ are from (*50*).

Ligand complex	R state		T state		Kinetic cooperativity		c^{-1}
	x'_R	x_R	x'_T	x_T	x'_R/x'_T	x_T/x_R	
$[Fe(II)O_2]^8$	α 59	12	2.9	1.8×10^2	20	15	300
	β 59	21	11.8	2.48×10^3	5	120	600
$[Fe(II)NO]^7$	25	10^{-5}	25	10^{-3}	1	100	100
Representative value (bent)	40		10		4	100	400
$[Fe(II)CO]^6$	6.5	10^{-2}	9×10^{-2}	0.1	72	10	720
$[Mn(II)NO]^6$	0.6	10^{-3}	3×10^{-2}	$\sim 10^{-2}$	20	10	200
Representative value (linear)	2		5×10^{-2}		40	10	400
Ratio x'_{bent}/x'_{linear}	20		200				

erably larger in the former than latter.

4) The effects of steric hindrance are manifested largely in the ligand association rate constants.

5) The absolute magnitude of the ligand dissociation rate constants is under electronic control, although there is an additional steric factor in the T state arising from nonbonded heme interactions and ligand-globin interactions.

6) The distribution of kinetic cooperativity between the association and dissociation reactions differs for linear and bent ligands.

That is, there is not a *single* molecular process that controls ligand affinity in hemoglobin. Rather, a more complicated mechanism is operative where the effects of quaternary structure, ligand geometry, and chain differences modulate nonbonded heme interactions and steric hindrance to ligand binding, and hence determine the rate and equilibrium constants. Some of these conclusions have been arrived at previously, and discussed from the viewpoint of elementary transition state theory (*16, 32*). Our present structural data give considerable force to these arguments.

Kinetic data for a number of single-chain heme proteins and some free hemes (Table 3), and corresponding data (Table 4) for human hemoglobin are summarized according to an allosteric viewpoint. In both tables, data are grouped according to whether the externally unconstrained heme-ligand complex is linear or bent. Striking correlations with ligand geometry are immediately evident.

Association Rate Constants

In the reactions of free hemes where distal steric hindrance is presumably absent, the ratio of the association rate constants for bent and linear ligands, x'_{bent}/x'_{linear}, is small, ranging from 1.5 to 8 (Table 3). For monomeric heme proteins (Table 3) and R-state human hemoglobin (Table 4), x'_{bent} is comparable with that for free hemes, but x'_{linear} is lower; the ratio x'_{bent}/x'_{linear} is consequently larger, ranging from 10 to 80 with a mean of about 20. We suggest that this rate ratio has a direct structural basis: the distortion of the heme-ligand complex observed in the stable structures of CO Hb, CO Mb, and CO erythrocruorin (and also cyanide metHb and cyanide metMb) is also present in the transition states for the association reactions; and the energy required for this distortion is reflected in an increased apparent free energy of activation for linear complexes of RT ln 20 = 1.8 kcal/mole (R, gas constant, and T, absolute temperature) over that for bent complexes, where little such distortion is observed. That is, steric hindrance lowers the association rate constant for linear ligands but has little effect on bent ligands.

For deoxyHb in the T state, this kinetic distinction between bent and linear ligands is even more marked (Table 4). The value of x'_{bent} is now slightly lower, and x'_{linear} much lower, than the corresponding values for free hemes or R-state hemoglobin. The ratio x'_{bent}/x'_{linear} is increased further, to around 200, corresponding to an increased apparent free energy of activation for linear complexes of 3.2 kcal/mole over that for bent complexes. These diminished association rate constants may arise from slight steric hindrance to bent ligand binding and from particularly stringent steric hindrance to linear ligand binding in deoxyHb, as is suggested by the x-ray results (*22*). Stress on the heme evidently has only a minor effect on the association rate constants of hemoglobin, since these are identical for the T and R states for NO and similar for the β chain for O_2. However, in model compounds the effects of stress can diminish association rate constants by up to an order of magnitude (*33, 34*).

With the exception of that for O_2, the kinetic data in Table 4 take no account of chain differences, which are small or absent in the reactions with CO and NO (*35*). Sawicki and Gibson (*36*) suggest that, contrary to previous findings, chain differences in the reaction with O_2 may be large in the T quaternary structure, up to a factor of 4 in the association reactions and 12 in the dissociation reactions. Although the assignment of kinetic components to individual chains is tricky, it appears that the β chains have higher association and dissociation rate constants than the α chains. That is, the β chains equilibrate more rapidly than the α chains with O_2 and with bulkier isonitriles (*37, 38*).

The above analysis and that of Szabo (*32*) relied solely on observed rate constants, treating ligand binding as though it were a single-step process. However, a highly detailed kinetic study of O_2 and CO binding to deoxyMb over a wide range of temperature (*39*) revealed more complicated kinetic behavior, which was interpreted in terms of several sequential microscopic steps and potential barriers in the overall reaction. For CO, there were four barriers, the central two of which were identified with protein-dependent effects, since they were absent

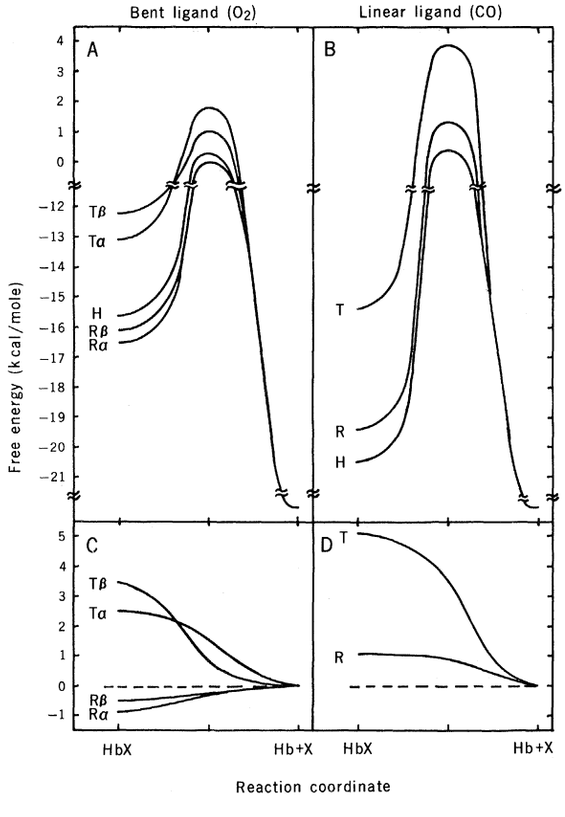

Fig. 4. Simplified profiles of free energy as a function of the reaction coordinate for the binding of bent ligands such as O_2 (A and C) and linear ligands such as CO (B and D) to the T and R states of hemoglobin, and to a free heme, denoted H. Although the true profiles are unknown, it is likely that they are more complicated, resembling those shown for myoglobin in figure 20 of (*39*). For hemoglobin, data were taken from Table 4, with $\gamma = 10^{13}$ sec^{-1}. For the heme, the following values were used: $x'_{O_2} = 45\ \mu M^{-1}$ sec^{-1}, $x_{O_2} = 32$ sec^{-1}, $x'_{CO} = 30\ \mu M^{-1}$ sec^{-1}, $x_{CO} = 8 \times 10^{-3}$ sec^{-1}. Considerable variation from heme to heme has been found, depending on the nature of the heme, the proximal base, and the solvent. For illustrative purposes, the free energies of all the unliganded species have been set equal; in fact, the unliganded T and R states differ in free energy by RT ln L, where L is the allosteric constant. (A and B) The reaction profiles for O_2 and CO; (C and D) the net reaction profiles obtained by subtracting the heme profiles from the hemoglobin profiles.

in the reaction of CO with free heme (*40*). For O_2, one of the central barriers was absent. It can be shown (*41*) that at room temperature the kinetic differences between O_2 and CO binding to deoxyMb arise not from differences in the number of barriers or in the properties of the inner and outer barriers, but solely from differences in the properties of the protein-dependent barriers separating states B and C [figure 20 in (*39*)]. This may be correlated with the distortion of the heme-ligand complex and the ligand pocket in CO Hb and CO Mb. Similar kinetic behavior will probably be found in the R and T states of hemoglobin, and these more complex results will also be capable of explanation in structural terms.

Ligand association rate constants are thus largely controlled by steric hindrance arising from nonbonded ligand-globin interactions. Indeed, the electronic properties of the heme have no effect on the CO association rate constants of hemoglobin (*42*) and hemes (*43*). It is not necessary to invoke nonbonded heme interactions to account for differences in association rate constants to deoxyHb.

Dissociation Rate Constants

In contrast to the association reaction, no such distal steric constraints are evident in the dissociation reaction; the dissociation rate constants vary over six orders of magnitude from ligand to ligand, with no obvious dependence on ligand geometry (Tables 3 and 4). In particular, distortion of the R-state CO complexes in heme proteins does not result in an increase in the dissociation rate constant for CO (Table 3) relative to free heme; evidently the liganded structure and the transition state are destabilized to roughly the same extent by this distortion. In certain model compounds, stress on the heme increases dissociation rate constants for O_2, but not for CO (*33, 34*).

Studies of ligand dissociation rates from hemoglobin (*42*) and myoglobin (*44*) reconstituted with hemes differing in their electronic properties through variation in the 2- and 4-substituents of the heme show that these rates are controlled almost entirely by the electronic properties of the iron-ligand bond; rupture of this bond is the rate-determining step in the overall dissociation reaction (*39, 42*). The explanation for the wide range in dissociation rate constants between ligands must therefore be sought in those electronic and structural factors that contribute to the stability of the iron-ligand bond, about which less is known at present.

Kinetic Cooperativity

A further correlation with ligand geometry is evident when kinetic cooperativity, expressed as x'_R/x'_T in the association reaction and x_T/x_R in the dissociation reaction, is considered (Table 4) (*35*). For bent complexes, kinetic cooperativity is concentrated in the ligand dissociation reaction: $x'_T/x'_R \sim 4$ but $x_T/x_R >> 1$. For linear complexes, kinetic cooperativity is more evenly distributed between the association and dissociation reactions, with a slight preference in favor of the association reaction; x'_R/x'_T and $x_T/x_R > 1$. The overall cooperativity, c^{-1}, expressed as $(x'_R/x'_T)(x_T/x_R)$ or as X_T/X_R, is similar in bent and linear complexes; merely its distribution differs.

It is striking that for the bent ligands NO and O_2 in the β chains, the kinetic cooperativity in the dissociation reaction x_T/x_R is almost identical, about 100, despite the six orders of magnitude difference in the dissociation rate x_T (and x_R) between NO and O_2. It is possible that this factor of 100 arises largely from nonbonded heme interactions, which are present in the T quaternary structure but absent in the R quaternary structure. However, these cannot be the sole contributor since, as noted above, their magnitude appears to be larger in the α chain than in the β chain (*29, 30*). This further emphasizes the unusual kinetic properties of the α chain toward O_2 (*38*).

All the above kinetic arguments may equally well be illustrated in free energy terms (*16*). In Fig. 4, A and B, we present the reaction profiles for O_2 and CO binding to hemoglobin, derived directly from the kinetic data in Table 4, and profiles typical of a model heme. In order to separate the protein-dependent effects from purely electronic effects of bond making and bond breaking, in Fig. 4, C and D, we show the reaction profiles that result when the model heme profile is subtracted from the corresponding hemoglobin profile. Deviations from the zero of free energy thus arise from the two purely protein-dependent processes, nonbonded ligand-globin interactions and nonbonded heme interactions, which alter the free energies of the transition states and liganded states.

The difference in free energy of the transition state between R and T may thus contain contributions from both processes. On the basis of our structural results and the kinetic results, we note that differences in this quantity between ligands arise almost entirely from the first process, nonbonded ligand-globin interactions. Similarly, the difference in free energy of the final liganded complexes between R and T contains contributions from both processes. We further note that the contribution of the first process to this differs for different ligands.

Thus, although different ligands have similar free energies of cooperativity, $-RT \ln c$, the relative contributions of the two molecular processes, nonbonded ligand-globin interactions and nonbonded heme interactions, to this free energy may differ significantly for different ligands. The molecular mechanism by which the binding of ligand brings about those changes in tertiary structure which lead to the change in quaternary structure thus differs in detail for different ligands.

References and Notes

1. Abbreviations used: Hb, hemoglobin; Mb, myoglobin; metHb, methemoglobin; NO Hb, nitrosyl hemoglobin; CO Hb, carbon monoxide hemoglobin. T and R denote the deoxy and liganded forms of Hb, in the allosteric notation.
2. J. M. Baldwin and C. Chothia, *J. Mol. Biol.* **129**, 175 (1979).
3. A. Warshel, *Proc. Natl. Acad. Sci. U.S.A.* **74**, 1789 (1977).
4. B. R. Gelin and M. Karplus, *ibid.*, p. 801.
5. M. F. Perutz, *Nature (London)* **228**, 726 (1970); *ibid.* **237**, 495 (1972).
6. We distinguish two types of nonbonded interactions involving the heme: interactions between the heme atoms and the iron ligands (proximal imidazole and the sixth ligand), referred to by Warshel (*3*) as 1-3 interactions and defined by us as *nonbonded ligand-heme interactions*; and interactions between the peripheral heme atoms and the globin, extensively discussed by Gelin and Karplus (*4*) and defined by us as *nonbonded heme-globin interactions*. We refer to these two types collectively as *nonbonded heme interactions*. A third type of nonbonded interaction, between the atoms of the sixth iron ligand and the surrounding globin, forms a major topic of this article; we denote it *nonbonded ligand-globin interaction. Tension at the heme* was described (*5*) as the constraints imposed by the T quaternary structure on the unliganded hemes, which increase the bond lengths between the iron atoms and their six ligands and lower the ligand affinity by opposing the change to the low spin, liganded state. *Kinetic cooperativity* is present in both ligand association and dissociation reactions. In the former, it is defined as the ratio of the second-order ligand association rate constants to the R and T states, denoted x'_R/x'_T; in the latter, as the ratio of the first-order ligand dissociation rate constants of the T and R states, denoted x_T/x_R. The product of the kinetic cooperativities in the association and dissociation reactions $(x'_R/x'_T)(x_T/x_R)$ is equal to K_T/K_R or c^{-1} in the allosteric notation. This relates the two kinetic cooperativities to the *equilibrium cooperativity*. We use the terms *stress* and *strain* as used in mechanics: application of stress to an object leads to strain, deformation of its structure. Crystallographic results only reveal strain, by comparison of observed bond lengths and angles with those found in (presumably unconstrained) model compounds; conversion of strain to stress and estimation of strain energies requires that the force constants for bond length or bond angle deformation be known.
7. J. F. Deatherage, R. S. Loe, C. M. Anderson, K. Moffat, *J. Mol. Biol.* **104**, 687 (1976).
8. J. F. Deatherage, R. S. Loe, K. Moffat, *ibid.* **104**, 723 (1976).
9. J. F. Deatherage and K. Moffat, *ibid.*, in press.
10. J. F. Deatherage, S. K. Obendorf, K. Moffat, *ibid.*, in press.
11. R. C. Ladner, E. J. Heidner, M. F. Perutz, *ibid.* **114**, 385 (1977).
12. E. J. Heidner, R. C. Ladner, M. F. Perutz, *ibid.* **104**, 707 (1976).
13. Our structural analysis is based on inspection of a series of complicated difference Fouriers (*7-10*). Quantification of the structural differences among the liganded hemoglobins requires crystallographic refinement of all their

structures, similar to that carried out on acid metHb (*11*). Although our interpretation is deliberately conservative, until such refinement is conducted it must be regarded as qualitative.
14. R. Henderson and K. Moffat, *Acta Crystallogr. Sect. B* **27**, 1414 (1971).
15. M. F. Perutz, J. E. Ladner, S. R. Simon, C. Ho, *Biochemistry* **13**, 2163 (1974); M. F. Perutz, A. R. Fersht, S. R. Simon, G. C. K. Roberts, *ibid.*, p. 2174; M. F. Perutz, E. J. Heidner, J. E. Ladner, J. G. Beetlestone, C. Ho, E. F. Slade, *ibid.*, p. 2187; M. F. Perutz, *Br. Med. Bull.* **32**, 195 (1976); *Annu. Rev. Biochem.* **48**, 327 (1979).
16. J. F. Deatherage, thesis, Cornell University (1978).
17. W. S. Caughey, R. A. Houtchens, A. Lanir, J. C. Maxwell, S. Charache, in *Biochemical and Clinical Aspects of Hemoglobin Abnormalities*, W. S. Caughey, Ed. (Academic Press, New York, 1978), p. 29; M. E. Johnson and C. Ho, *Biochemistry* **13**, 3653 (1974); S. Ogawa, R. G. Shulman, M. Fujiwara, T. Yamane, *J. Mol. Biol.* **70**, 301 (1972); R. B. Moon, K. Dill, J. M. Richards, *Biochemistry* **16**, 221 (1977); T. G. Spiro, J. D. Stong, P. Stein, *J. Am. Chem. Soc.* **101**, 2648 (1979).
18. J. H. Enemark and R. D. Feltham, *Coord. Chem. Rev.* **13**, 339 (1974).
19. J. L. Hoard, in *Porphyrins and Metalloporphyrins*, K. M. Smith, Ed. (Elsevier, Amsterdam, 1976), p. 317. Structural data on unliganded and oxygenated model hemes is also provided by G. B. Jameson, F. S. Molinaro, J. A. Ibers, J. F. Collman, J. I. Brauman, E. Rose, K. S. Suslick [*J. Am. Chem. Soc.* **100**, 6769 (1978)].
20. R. Hoffman, M. M.-L. Chen, D. L. Thorn, *Inorg. Chem.* **16**, 503 (1977).
21. P. Bretscher, thesis, Cambridge University, (1968); J. C. Norvell, A. C. Nunes, B. P. Schoenborn, *Science* **190**, 568 (1975); R. Huber, O. Epp, H. Formanek, *J. Mol. Biol.* **52**, 349 (1970); W. A. Hendrickson and W. E. Love, *Nature (London) New Biol.* **232**, 197 (1971). A preliminary structure for oxyMb has been presented by S. E. V. Phillips [*Nature (London)* **273**, 247 (1978)] and for oxyerythrocruorin by E. Weber, W. Steigemann, T. A. Jones, R. Huber [*J. Mol. Biol.* **120**, 327 (1978)]. A highly detailed comparison of the structures of liganded erythrocruorins has just appeared: W. Steigemann and E. Weber, *J. Mol. Biol.* **127**, 309 (1979).
22. G. Fermi, *J. Mol. Biol.* **97**, 237 (1975).
23. T. Mashiko, M. E. Kastner, K. Spartalian, W. R. Scheidt, C. A. Reed, *J. Am. Chem. Soc.* **100**, 6354 (1978); W. R. Scheidt, I. A. Cohen, M. E. Kastner, *Biochemistry* **18**, 3546 (1979).
24. T. Takano, *J. Mol. Biol.* **110**, 537 and 569 (1977).
25. In all four molecules distortion of the hemes from planarity was investigated by constraining the pyrroles to tilt as rigid units about a line passing through adjacent methene carbons (or a line parallel to it, passing through C-1 and C-2 of the pyrroles). That is, the four methene carbons were constrained to remain coplanar throughout the refinement. Ruffled geometries such as S_4 and D_{2d}, in which the methene carbons lie alternately above and below the mean porphyrin plane, were not accessible to the refinement, but regular (and irregular) domed geometries were. This constraint may have been too restrictive. Hoard (*19*) has emphasized ". . . a generally superior pattern of σ bonding should be afforded by a marked D_{2d} ruffling of the core in those metalloporphyrins wherein the complexing metal-pyrrole nitrogen bonds are significantly stretched from the lengths preferred with nitrogen atoms of monodentate ligands." That is, stress at the heme core is frequently relieved by ruffling of the porphyrin.
26. Tilting of the heme occurs in conjunction with increased ligand bulk and decreased iron spin, and involves change in orientation of the porphyrin plane between the E and F helices to a position more inclined to them and to the molecular diad axis (Fig. 3). Heme tilt has been observed in many other difference Fouriers [see discussion in (*9*) and references cited therein].
27. L. Anderson, *J. Mol. Biol.* **79**, 495 (1973); *ibid.* **94**, 33 (1975).
28. P. Eisenberger, R. G. Shulman, B. M. Kincaid, G. S. Brown, S. Ogawa, *Nature (London)* **274**, 30 (1978).
29. M. F. Perutz, J. V. Kilmartin, K. Nagai, A. Szabo, S. R. Simon, *Biochemistry* **15**, 378 (1976); J. C. Maxwell and W. S. Caughey, *ibid.*, p. 388. An estimate of the free energy associated with spin change is given by C. Messana, M. Cerdonio, P. Shenklin, R. Noble, G. Fermi, R. N. Perutz, M. F. Perutz, *ibid.* **17**, 3652 (1978).
30. Y. Sugita, *J. Biol. Chem.* **250**, 1251 (1975).
31. D. W. Seybert, J. F. Deatherage, K. Moffat, *Biophys. J.* **17**, 235a (1977).
32. A. Szabo, *Proc. Natl. Acad. Sci. U.S.A.* **75**, 3108 (1978).
33. V. S. Sharma, J. F. Geibel, H. M. Ranney, *ibid.*, p. 3747.
34. D. K. White, J. B. Cannon, T. G. Traylor, *J. Am. Chem. Soc.* **101**, 2443 (1979).
35. V. S. Sharma, M. S. Schmidt, H. M. Ranney, *J. Biol. Chem.* **251**, 4267 (1976); R. Hille, G. Palmer, J. S. Olson. *ibid.* **252**, 403 (1977).
36. C. A. Sawicki and Q. H. Gibson, *ibid.* **252**, 7538 (1977).
37. J. S. Olson and C. Binger, *Biochim. Biophys. Acta* **434**, 428 (1976).
38. This illustrates the difficulty of accounting for kinetic results in structural terms. In deoxyHb the ligand binding site of the β chain is largely occluded by the side chain of Val E11, but that of the α chain is more open. It might therefore be anticipated (*5*) that the α chains would equilibrate more rapidly with ligand, contrary to the kinetic results. The discrepancy probably lies in our inability at present to estimate the free energy associated with ligand pocket opening. Although the equilibrium position favors the occluded conformation, the kinetic results suggest that a more open conformation is readily accessible. The molecular basis for the kinetic chain differences with O_2 remain a puzzle [see (*33*)]. However, it is possible that the kinetic results are in error, and that the chain identification should be reversed. This would improve agreement both with the deoxyHb structure, and with our kinetic model.
39. R. H. Austin, K. W. Beeson, L. Eisenstein, H. Frauenfelder, I. C. Gunsalus, *Biochemistry* **14**, 5355 (1975).
40. N. Alberding, R. H. Austin, S. S. Chan, L. Eisenstein, H. Frauenfelder, I. C. Gunsalus, T. M. Nordlund, *J. Chem. Phys.* **65**, 4701 (1976).
41. From equation 47 of (*39*), in the high-temperature limit the CO association rate constant λ_{1V}^{CO} is given by, in the notation of (*39*),

$$\lambda_{1V}^{CO} = k_{ba}^{peak}(k_{cb}k_{dc}k_{ed})/(k_{bc}k_{cd}k_{de})$$
$$= k_{ba}^{peak}K_bK_cK_d$$
$$= \text{(rate constant for the transition from well B} \rightarrow \text{A) times the product of preceding equilibrium constants.}$$

By analogy, the corresponding O_2 association rate constant is then

$$\lambda_{1V}^{O_2} = k_{ba}^{peak}(k_{ec}k_{cb})/(k_{ce}k_{bc})$$
$$= k_{ba}^{peak}K_eK_b$$

Now from the data in table 1 of (*39*), $k_{ba}^{peak}(O_2) = 1.2\ k_{ba}^{peak}(CO)$; $K_c(O_2) = 1.1\ K_cK_d(CO)$; and $K_b(O_2) = 32\ K_b(CO)$. That is, the kinetic differences between O_2 and CO binding to deoxyMb at high temperature (310 K) are revealed solely in K_b, the equilibrium constant describing the transition between the protein-dependent wells B and C. Szabo's assumption (*32*) that heme proteins control the kinetics largely by modulating the height of the barrier closest to the heme (separating wells A and B) evidently does not apply to the kinetic distinction between O_2 and CO.
42. D. W. Seybert, K. Moffat, Q. H. Gibson, C. K. Chang, *J. Biol. Chem.* **252**, 4225 (1977).
43. A. Berzinis and T. G. Traylor, unpublished results [quoted by White *et al.* (*34*)].
44. M. Sono, P. D. Smith, J. A. McCray, T. Asakura, *J. Biol. Chem.* **251**, 1418 (1976).
45. E. Antonini and M. Brunori, *Hemoglobin and Myoglobin in Their Reaction with Ligands* (Elsevier, New York, 1971), tables 9.2, 9.4, and 11.6.
46. E. Moore and Q. H. Gibson, *J. Biol. Chem.* **251**, 2788 (1976); R. Cassoly, *J. Mol. Biol.* **98**, 581 (1975); ——— and Q. H. Gibson, *ibid.* **91**, 301 (1975).
47. H. Yamamoto, F. J. Kayne, T. Yonetani, *J. Biol. Chem.* **249**, 691 (1974).
48. C. K. Chang and T. G. Traylor, *Proc. Natl. Acad. Sci. U.S.A.* **72**, 1166 (1975); J. Geibel, J. Cannon, D. Campbell, T. G. Traylor, *J. Am. Chem. Soc.* **100**, 3575 (1978); T. G. Traylor, C. K. Chang, J. Geibel, A. Berzinis, T. Mincey, J. Cannon, *ibid.*, in press; T. G. Traylor, D. Campbell, V. Sharma, J. Geibel, *ibid.* **101**, 5376 (1979).
49. C. A. Sawicki and Q. H. Gibson, *J. Biol. Chem.* **251**, 1533 (1976); *Biophys. J.* **24**, 21 (1978).
50. Q. H. Gibson, personal communication.
51. Supported by NSF grants GB 32231X and PCM75-02366, and by NIH grant HL 18309 (K.M.); and by NSF predoctoral fellowship (D.W.S.). We thank Quentin Gibson and Lynn Hoard for helpful discussions, and W. R. Scheidt and T. G. Traylor for communicating unpublished results.